Research Article ISSN 2639-8478

Cancer Science & Research

Simulation of the nIORT® Treatment by Fast Neutrons of Severe Brain Cancers (as GBM) and Comparison with Standard IORT Techniques Adopting X-rays and Electrons

Martellini M[1]*, Sarotto M[2], Ferrari P[3], Giuseppe Gherardi[1] and Marco Venturi[4]

[1]*TheranostiCentre S.r.l., Via Freguglia 8 – 20122 Milan, Italy.*

[2]*ENEA NUC-ENER-PRO, CR Saluggia, Strada per Crescentino 41 – 13040 Saluggia, Italy.*

[3]*ENEA Radiation Protection Institute, Via dei Mille 21 – 40121 Bologna, Italy.*

[4]*Medical Consultant of TheranostiCentre S.r.l., Via Freguglia 8 – 20122 Milan, Italy.*

***Correspondence:**
Martellini M, TheranostiCentre S.r.l., Via Freguglia 8 – 20122 Milan, Italy.

Received: 11 Jan 2025; **Accepted:** 20 Feb 2025; **Published:** 28 Feb 2025

Citation: Martellini M, Sarotto M, Ferrari P, et al. Simulation of the nIORT® Treatment by Fast Neutrons of Severe Brain Cancers (as GBM) and Comparison with Standard IORT Techniques Adopting X-rays and Electrons. Cancer Sci Res. 2025; 8(1): 1-15.

ABSTRACT

This work investigates the feasibility of using fast neutrons for intra-operative radiotherapy (nIORT®) in the treatment of aggressive brain cancers, particularly glioblastoma multiforme (GBM). A compact neutron generator produces neutrons of 2.45 MeV energy with high linear energy transfer, elevated relative biological effectiveness (RBE ≅3÷5 times higher than X-rays and electrons) and reduced oxygen enhancement ratio, key factors in overcoming hypoxia-mediated radioresistance. Monte Carlo simulations using the MCNP code demonstrate that the nIORT® device can deliver a diffuse high-flux beam (~10^8 cm^{-2} s^{-1}), achieving equivalent dose rates of ~1.2 Gy(RBE)/min and allowing short irradiation times. Unlike standard IORT techniques relying on focused beams of X-rays or electrons, the diffuse neutron beam can treat large and topographically irregular tumor beds, a notable advantage in GBM. The dose gradient in tissues depth induced by fast neutrons exhibits complementary features with respect to the steep behavior of electrons and the more penetrating X-rays, that could be advantageously exploited in balancing the need for an effective local tumor control.

The compactness and limited weight (~120 kg) of the self-shielded nIORT® device remotely operated via a robotic arm, and its ability to administer high dose targets within few minutes, represent fundamental advantages in the view of possible treatments in a hospital OR dedicated to nIORT® without posing safety concerns. Although the nIORT® approach requires specialized equipment, personnel, and careful logistical planning, its enhanced efficacy and broader dose coverage suggest a significant potential in adjuvant therapy. Combining nIORT® with immunotherapy warrants further study, as fast-neutron–induced cell death could intensify immune responses and support synergistic effects of immune checkpoint inhibitors. If clinically validated, nIORT® may offer an important step toward more effective, multimodal treatment strategies - integrating surgery, chemotherapy, and immunotherapy - to improve outcomes for patients with GBM and other high-risk brain malignancies.

Keywords

Brain cancers (GBM), neutron-Intraoperative radiation therapy (nIORT®), Standard IORT techniques, Dosimetry parameters.

List of Abbreviations

CNG: Compact neutron generator, CSC: Cancer Stem Cell, DD: Deuterium-deuterium, DSB: Double strand break, EBRT: External beam radiotherapy, EMT: Epithelial–mesenchymal transformation, GBM: Glioblastoma multiforme, HDPE: High density polyethylene, ICI: Immune-checkpoints inhibitor, IORT: Intraoperative radiation therapy, IOERT: Electron IORT, LET: Linear energy transfer, LEX-IORT: Low energy X-rays IORT, LTC: Local tumor control, MCNP: Monte Carlo N-particle, NHEJ: Nonhomologous end joining, nIORT®: Neutron IORT, OAR: Organ at risk, OER: Oxygen enhancement ratio, OR: Operating

room, QCC: Quiescent cancer cell, RBE: Relative Biological Effectiveness, RIAE: Radiation-induced abscopal effect, RIBE: Radiation-induced bystander effect, RISM: Radiation-induced secondary malignancy, RT: Radiation therapy, SSB: Single strand break, TME: Tumor microenvironment, TMZ: Temozolomide.

Symbols

D'_f	Physical dose rate [Gy min^{-1}]
D'_{eq}	Equivalent dose rate [Gy (RBE) min^{-1}]
$D_{eq,T}$	Equivalent dose Target (or clinical end-point) [Gy (RBE)]
φ	Flux [cm^{-2} s^{-1}]
min	minute(s)
TT	Treatment time

Introduction

Brain tumors, particularly glioblastoma multiforme (GBM), are known for their high aggressiveness and the lack of curative treatment options. The GBM is the most common and deadliest primary malignant brain tumor in adults, characterized by rapid growth, high invasiveness and a remarkable resistance to conventional therapies. Despite advances in surgical, chemotherapy, and radiotherapy (RT) techniques, the prognosis for GBM patients remains poor, with a median survival of approximately 12÷15 months following diagnosis [1]. One of the defining features of GBM is its diffuse infiltration into surrounding brain tissue, which makes complete surgical resection nearly impossible. Even with maximal tumor removal, residual microscopic disease typically persists, contributing to high recurrence rates. Additionally, GBM exhibits large tumor beds (~4÷10 cm) and significant heterogeneity at the cellular and molecular levels, further complicating treatment efforts. This heterogeneity includes variations in genetic mutations, metabolic pathways and responses to therapy, which collectively contribute to the tumor's resilience against standard treatments [2,3]. The current standard of care for GBM is a combination of surgery, RT and chemotherapy, commonly referred to as the "Stupp protocol". This chemoradiation therapy regimen involves maximal safe surgical resection of the tumor, followed by RT (typically 60 Gy delivered in 30 fractions) combined with concurrent daily administration of temozolomide (TMZ), an oral alkylating chemotherapy agent. After the RT phase, patients continue with adjuvant TMZ for six cycles. This protocol has demonstrated modest improvements in overall survival and progression-free survival: nearly all patients experience disease progression due to the tumor's intrinsic resistance mechanisms [4].

Determining the most efficient type of radiation remains a critical question in the RT research field. As well known, biological responses triggered by RT exposure mainly depend on:

- the energy deposition per unit length of radiation track, i.e., linear energy transfer (LET: keV/μm), that is directly proportional to the number of ionization events along the particles' path;
- the relative biologic effectiveness (RBE), representing the ratio of doses required by two different radiations (e.g., photons and ions) to cause the same level of biologic effect, in which photon X and γ-rays of certain energy are assumed as reference radiation with a unitary RBE value.

Recent advancements have explored the use of radiation particles with high LET for GBM treatment, such as neutrons and carbon ions [5]. While X-rays and electrons are commonly used due to their accessibility and established protocols, high-LET particles such as neutrons, protons and carbon ions have shown promising results in achieving better tumor control. Proton therapy, for instance, allows precise dose delivery with minimal exposure to surrounding healthy tissues, making it an attractive option for complex tumors. Carbon ion therapy combines the advantages of proton therapy with the high biological effectiveness of high-LET radiation, potentially offering even greater benefits [6].

When compared to conventional low-LET radiation, high-LET particles offer superior biological effectiveness (i.e., RBE strongly depending on LET value) since they generate fewer but larger double-strand DNA breaks (DSBs) per unit dose. Apart from LET, the RBE value is also affected by the dose per fraction (inversely proportional), the type of tissue and the cell cycle stage (the radio-sensitivity change at different stages). In any case, irradiation particles with low LET and RBE values (as X-rays) are less effective in treating radioresistant tumors, such as GBM, and may require higher doses to achieve the same therapeutic effect, increasing the risk of damaging healthy tissues. Otherwise, radiation particles with high LET and RBE (as fast neutrons) cause more complex DNA damage, which is harder for tumor cells to repair, potentially improving the local tumor control (LTC) and patient outcomes. Early clinical studies and preclinical data suggest that high-LET RT could significantly enhance the treatment response in radioresistant tumors like GBM: further research is required to optimize treatment protocols and minimize toxicity to surrounding healthy tissues [7].

In parallel with RT, immunotherapy is gaining attraction as a complementary strategy for the GBM treatment. The immunosuppressive tumor microenvironment (TME) of the GBM has historically hindered the effectiveness of immunotherapies, such as immune checkpoint inhibitors (ICIs). But recent studies suggest that combining RT with immunotherapy could help overcome this barrier. Radiation-induced tumor cell death releases neoantigens, which can enhance the immune system's ability to recognize and target cancer cells. Early-phase clinical trials are currently investigating combinations of RT and immunotherapy, including vaccines, ICIs and adoptive cell therapies, showing promising preliminary results [8]. Given the complexity of GBM, a multimodal approach that integrates surgery, chemoradiation, advanced RT techniques and immunotherapy may represent the best path forward. Continued research into these complementary strategies is critical to improving survival and quality of life for patients with this devastating disease [9].

Among the advanced RT techniques, the intra-operative

radiotherapy (IORT) has become a very promising adjuvant treatment [10]. As a meaningful example, in the case of breast cancer some studies demonstrate both feasibility and outcome equivalence, if not superiority when applied in the optimal setting, respect to the external beam radiotherapy (EBRT) [11]. In the IORT treatment plannings the dose target is administered in a one-shot irradiation directly in the surgical cavity (and not by a fractionation scheduled EBRT on the skin upon the "closed wound") by zeroing the time to initiation that limits the repopulation of residual cancer cells in the TME. Therefore, the one-shot IORT irradiation - with craniotomy after maximal surgical resection, aiming to avoid the tumor cells' proliferation between surgery and radio-chemotherapy, and to spare healthy tissues - could represent a very promising therapeutic option to be inserted in a multimodal approach protocol for the treatment of the GBM and other severe brain cancers.

Some IORT techniques were recently investigated and adopted for the GBM treatment [12-18]. Generally, the most common techniques for the solid cancers' treatment mainly exploit as irradiation particles:

- low-energy (~50 keV) X-rays, with the so-called low energy X-rays IORT (LEX-IORT [13]);
- high-energy (~1÷5 MeV) electrons, with the so-called IOERT [16].

Even though the IORT treatments sometimes present favorable radiobiological factors and outcome data beyond those obtained with standard EBRT techniques, their applicability is still limited to some cancer pathologies and related tumor bed features. Besides the low effectiveness of low-LET and low-RBE particles in treating radioresistant cancers, the tumor beds with significant extension and topographic irregularities (as the GBM) remain a therapeutic challenge with existing technologies foreseeing a focused beam (as in the IOERT, most reliable for flat tissue surfaces) and/or a beam with a limited irradiation target area (as in the LEX-IORT).

This research study considers the IORT treatment of solid brain tumors with fast neutrons produced by a compact neutron generator (CNG) that, through the deuterium-deuterium (DD) fusion reaction, generates neutrons of 2.45 MeV energy [19]. The CNG is self-shielded, limited in size and weight (~120 kg) and manageable remotely by a robotic arm. The utilization of a compact source, instead of big installations as accelerators (producing neutrons e.g., by spallation process of the incident ions on beryllium or heavy metal targets) represents a fundamental advantage in the view of possible treatments in a hospital operating room (OR). Difficulties and limitations of the irradiation treatments made in the past with fast neutrons [20] should be mainly overcome by the IORT modality, also considering that the excessive toxicity of neutrons found by oncologists was partly due to inadequate radiobiological understanding, and it was possible to achieve better clinical outcomes with low-dose neutrons than photons [21].

Differently from the treatments with low-LET particles mainly inducing isolated DNA lesions and sublethal damage, the high-LET neutrons could induce highly localized and clustered DNA damage more difficult to repair, leading to necrosis and apoptosis of the cancer cells. Additionally, there are concurrent secondary effects leading to cancer cells' death, such as a major release of reactive oxygen (and nitrogen) species and free radicals. High-LET radiation can overcome multiple mechanisms of resistance typical of low LET radiation, including tumor hypoxia (that within the TME enhances resistance to RT) with the further advantage of a reduced oxygen enhancement ratio (OER) [22,23]. The RT with fast neutrons presents also some advantages in the treatment of slow-growing tumors (e.g., as GBM and prostate adenocarcinomas) and, thanks to the better therapeutic gain than photon therapy, it could be the most appropriate for the partially resected and recurrent cancers (e.g., as GBM and salivary gland tumors) [21].

As discussed in this article, the fast neutrons of 2.45 MeV energy produced by the CNG could be used for tumors irradiation. Both LET and RBE values depend on neutron energy and the biological tissue considered [24]: with energy of about 2.5 MeV, the LET results ~30÷50 keV/µm [25], the RBE in tumor cells was measured in the 4÷5 range and limited to about 2.5 in normal tissues [24]. Thus, the biological effectiveness of fast neutrons in tumor cells is about 4÷5 times the ones of standard LEX-IORT and IOERT techniques. In this work, the RBE was conservatively assumed equal to 3.5 [26] for all tissues of the surgical cavity potentially filled with quiescent cancer cells (QCCs).

Relying on the beneficial IORT peculiarities (time to initiation zeroing from surgical rejection, administration of high dose levels in the tumor bed and lower dose levels in neighboring normal tissue), this feasibility study investigates the brain cancers treatment by means of the so-called neutron-IORT (nIORT®) technique patented by the TheranostiCentre S.r.l. company (TC, Italy) [27]. Besides the high-LET and high-RBE of the fast neutrons, the spatial diffusion of the beam produced by the CNG can overcome some limitations of the current IORT techniques for tumor beds with significant extension and topographic irregularities, as in the case of GBM. Moreover, the almost isotropic distribution of the beam could be particularly suitable for the irradiation of the local recurrences, frequently observed within 2÷3 cm from the initial GBM lesion and representing the major cause for clinical deterioration (and deaths) [28].

The CNG performances for potential nIORT® treatments of brain cancers with craniotomy were analyzed by means of the Monte Carlo code MCNP ver. 6.1 [29] coupled with the most up to date ENDF/B-VIII.0 nuclear data [30]. By modelling a 4-cm-diameter cylindrical IORT applicator to be inserted in the "skull opening", the neutron flux distribution and the corresponding dosimetry parameters were evaluated in the superficial tissues of the surgical cavity (brain, skull and skin) and in brain depth. The MCNP code was also adopted to simulate the irradiation with standard IORT techniques adopting X-rays and electrons:

by maintaining the 4-cm-diameter cylindrical IORT applicator, a focused beam of 2-cm-diameter was assumed for both particles. 50 keV photons and 1 MeV electrons were considered for LEX-IORT and IOERT, respectively, usually adopted for treating superficial tumors with distinct advantages in terms of dose uniformity in the target volume [12-18]. This research study analyses - and remarks - the complementary features of the nIORT® potential treatments in comparison to the standard LEX-IORT and IOERT techniques, especially for what concerns the utilization of a diffuse beam of high LET and high RBE neutrons and its impact on the main dosimetry parameters, such as the flux/dose profiles in the superficial tissues of the surgical cavity and in brain depth.

The D-D Fusion Compact Generator for nIORT®

In the last 5 years, the research program on nIORT® was carried out by TC in collaboration with the Berkion Technology LLC company (BT, USA) and the Italian National Agency for New Technologies, Energy and Sustainable Economic Development (ENEA). The main outcomes of the activities are represented by:

- the fabrication of the first two prototypes of the DD-CNG (briefly described hereafter) in which the second one foresees some technological advancements making possible its potential installation in an OR dedicated to nIORT® treatments without posing safety and environmental concerns [31];
- the realisation of a new equipped ENEA laboratory [32] for the experimental characterization of the CNG prototypes and successive related experiments in view of the nIORT® application, e.g., *in vitro* tests on commercial cancer cells.

The CNG design was filed as an international patent in 2021 and registered at the WIPO (World Intellectual Property Organization) in 2023 [31]. The conceptual scheme in Figure 1 summarizes its main design features and shows its three main components:

- the ion source, that is a RF-driven plasma chamber with D (a nonradioactive isotope of hydrogen);
- the acceleration column made of High-Density Polyethylene (HDPE, having excellent properties in shielding neutrons);
- the beam target electrode made of titanium.

The two CNG prototypes - designed and developed in the collaborative research program by TC, BT and ENEA - were built in the BT laboratories in the last three years. The picture in the top-right part of Figure 1 shows the HDPE accelerator column (about 15 cm in diameter) and the attached RF plasma chamber. The positive deuterium ions (D+) created in the RF chamber are accelerated to the titanium target where DD fusion reactions occur by generating neutrons of 2.45 MeV energy. Operating the DD-CNG at 100 kV - 10 mA DC, a neutron yield of 3.3 10^9 s^{-1} is generated in the titanium target and the neutron flux results ~10^8 cm^{-2} s^{-1} at the irradiation window close to the target [31].

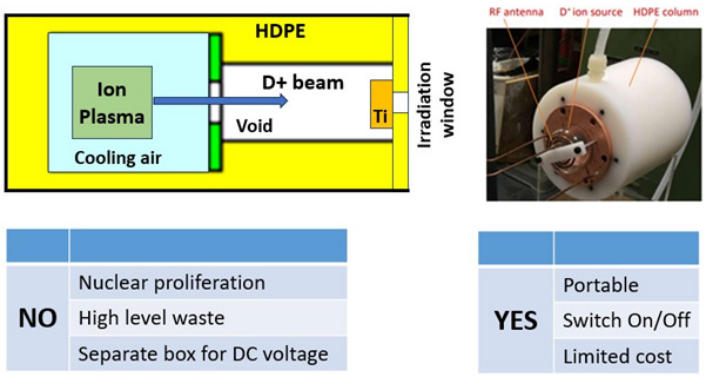

Figure 1: Conceptual design and main features of the D+ ion-based CNG. Picture of the HDPE accelerator column with the D+ ion source plasma chamber (top-right).

Dose Calculation Methodology for nIORT®

To simulate the nIORT® treatment with the MCNP code [29], the CNG model was positioned close to a head analytical model with craniotomy (see next section). The neutron flux levels in the brain surgical cavity were evaluated starting from the neutron yield (≅ 3.3 10^9 s^{-1}) generated by the 100 kV-10 mA DC D^+ ions impinging on the titanium target, with a near-isotropic direction of emission reproduced by the code. Neutrons are uncharged particles that do not interact with electrons clouds, but directly with target nuclei through scattering and absorption reactions. In human tissues, the most dominant process of energy transfer derives from the interaction with hydrogen nuclei (for their abundance, high cross-section and low mass compared to the other atoms) and mainly generates recoil protons. The MCNP simulations were not restricted to neutrons (*i.e.*, primary ones coming from the titanium target and secondary ones coming from the scattering with CNG components and patient tissues), but they also include photons: *i.e.*, gammas (γ) created by neutrons interaction with tissues' nuclei and CNG shielding.

The physical dose rate distributions (Gy/min) in the superficial tissues of the surgical cavity around the nIORT® applicator and in brain depth were evaluated with MCNP, that simulates accurately the interaction of neutrons and secondary photons in the tissues. Starting from the physical dose rates due to neutrons ($D'_{f,n}$) and gammas ($D'_{f,\gamma}$) expressed in Gy per minute (Gy/min), the total equivalent dose rate (D'_{eq}) administered - expressed in Gy (RBE)/min - can be obtained by the following equation:

$$D'_{eq} = RBE_{\gamma} \cdot D'_{f,\gamma} + RBE_{n} \cdot D'_{f,n} \text{ [Gy (RBE)/min]} \quad (1)$$

where:

- the RBE value of fast neutrons in biological tissues (RBE_n) varies between 3 and 5 [24-26] and here it was assumed 3.5 for all the tissues of the surgical cavity (brain, skull and skin);
- the RBE value of secondary photons in biological tissues (RBE_n) was assumed 1.1 [13].

The equivalent dose rate profiles due to neutrons and photons were calculated starting from the physical dose rates in the biological tissues calculated directly by MCNP, and then multiplied by the corresponding RBE values by equation (1). The neutrons' contribution to the total equivalent dose rate in superficial tissues results about 650 times higher than the contribution of secondary gammas because of the higher neutron flux (≅20x photon flux), LET and RBE (3.5 vs. 1.1) values. Referring to the aimed dose target ($D_{eq,T}$) defined by standard clinical protocols, usually named clinical end point, the treatment time (TT) needed to administer it can be easily obtained:

$$TT = D_{eq,T}/D'_{eq} \quad [\text{min}] \quad (2)$$

The spatial distributions of the equivalent dose rates (1) in the surgical cavity and in brain depth were accurately evaluated by MCNP to estimate the peak value administered in the superficial tissues at the center of the tumor bed - usually corresponding to the $D_{eq,T}$ clinical end point – as well as the dose administered in the surrounding tumor bed margins and normal tissues, whose compositions were retrieved from reliable MC human phantoms' models in literature [33].

Monte Carlo Simulation of the nIORT® Treatments

The left side of Fig. 2 shows a 2D section of the MCNP model of the CNG and surrounding shields, made of borated PE and an external layer of lead (mainly for γ rays). The whole system is a cylinder with about 30 cm in diameter and 40 cm in length. For simplicity, the MCNP model does not consider the ion source chamber (in the back part of the acceleration column, see Figure 1) since the simulations start from the (near isotropic) spatial distribution of the 2.45 MeV neutrons emitted from the titanium target on the opposite side of the CNG: thus, this model simplification has no impact on the flux and dose rate results into the biological tissues here presented. The right side of Figure 2 shows an enlarged drawing of the MCNP model of the cylindrical IORT applicator (in purple color), shaped around the HDPE bearing-ledge structure of the CNG containing an aluminum holder for the titanium target. The applicator pipe made of Lucite ($C_5O_2H_8$) is almost transparent for neutrons and, via hard-docking, can be inserted close to (or in contact with) the tumor bed inside the surgical cavity. For brain cancers irradiation, the IORT applicator was positioned in the skull "opening" surrounded by skin and skull tissues. The skull was modelled 0.7 cm thick and its covering skin 0.5 cm thick (> 0.3 cm [33] to consider "folds"). Actually, the tumor bed extension is not so well-delimited as in the MCNP model (with the net separation between the brain tumor bed and normal tissues): in any case, the flux and dose rate levels were accurately calculated / monitored in the small volumes of the MCNP cells modelling all the tissues around the applicator.

The right side of Figure 2 refers to an IORT applicator of 4 cm diameter and about 2 cm long: the air gap between the CNG walls and the patient's head skin results about 1 cm. A thin air gap (0.2 cm thick, light blue cell) was introduced between the applicator end-cap and the tumor bed, that is to consider an average distance between them for the "not uniform" contact due to tissue irregularities.

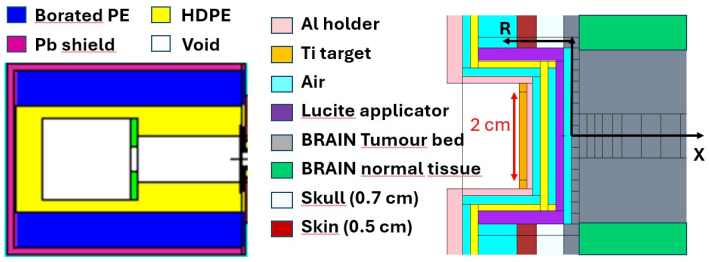

Figure 2: Vertical section of the MCNP model of the CNG and surrounding shields (left). Zoom section of the MCNP model of the 4-cm-diameter cylindrical applicator and surrounding surgical cavity simulating the nIORT® treatment of brain cancers (right).

In the following graphs - with flux and dose rate profiles in superficial and deep tissues - two reference directions are considered. As shown in the right part of Figure 2: the "X" axis is used for the depth inside the brain tumoral tissue, the "R" axis is used for the superficial tissues of the surgical cavity around the IORT applicator. To be remarked that "R" represents the distance between the center of the tumor bed (i.e., surface cell lying on the applicator symmetry axis) and the center of each MCNP cell representing the superficial tissues of the surgical cavity. With the cylindrical geometry, R corresponds to the brain tissues in front of the applicator end-cap until 2 cm, while bigger R values refer to the skull and skin cells on its lateral side.

The left side of Figure 3 shows the 2D spatial distribution of the neutron flux (expressed in cm^{-2} s^{-1}) near the IORT applicator obtained by the MCNP code. The neutron beam behaves like an ionizing radiation "foam" filling the surgical cavity and allows to irradiate the tumor bed margins, normally filled by potential QCCs, with lower - but still significant - dose levels. As expected, the flux peak in the surgical cavity (~10^8 cm^{-2} s^{-1}) is obtained at tissues surface at the center of the tumor bed (in correspondence of the IORT applicator symmetry axis), as evidently shown in the graph in the top-right part of Figure 3 where the flux values in the superficial tissues of the surgical cavity are represented. As indicated by the R axis in the right part of Figure 2, until 2 cm the flux values refer to brain tissues, while the last two ones refer to the skull and skin cells.

As shown in the bottom-right part of Figure 3, going in brain depth the flux level drops by one half in the first centimeter of tissue and decreases by a factor 5 at about 3 cm depth. The neutrons penetrate into tissues but, because of their high LET (~ 30÷50 keV/μm [25], or even higher [21,34]) and their diffuse spatial distribution, the overwhelming part of the dose is released at surface and in the first centimeters: the deep tissues are still irradiated by the thermal and epithermal tails of the neutron flux having decisively lower LET values, and hence significantly less effective in cell damaging. To be mentioned that in both superficial and deep flux profiles shown in Figure 3, the uncertainty of the MCNP results was not indicated:

their relative standard deviation is however lower than ~1%, as for the flux, physical and equivalent dose rate profiles shown in the next sections.

Dose Calculation Methodology for LEX-IORT and IOERT

The MCNP ver. 6.1 code (and ENDF/B-VIII.0 nuclear data) was adopted also to simulate LEX-IORT and IOERT irradiation treatments. Differently from neutrons, both X-rays and electrons interact with the electrons clouds. The X-rays radiation with low LET – ~4 keV/μm at 50 keV energy [35,36] - has a significant power of penetration, as the secondary electrons produced deposit their energy over large distances in the tissues. Coherently, the MCNP simulations were not restricted to the primary photons and included the secondary electrons created by X-rays interaction with the tissues, e.g. through the Compton and photoelectric effects.

Differently from neutrons and X-rays, the electrons are directly ionizing particles that can disrupt the atomic structure of the target by producing chemical and biological changes. The electron radiation has relatively high LET – up to ~10 keV/μm at 1 MeV energy [35,36] – and the beam deposits its energy at shorter distances. Indeed, as electrons travel through a medium, they interact with atoms by a variety of processes owing to Coulomb force interactions. In low-atomic-number media such as water or tissues, electrons lose energy predominantly through inelastic collisions with atomic electrons creating ionization/excitation events. In higher-atomic-number materials, such as lead, inelastic collisions with atomic nuclei (i.e., bremsstrahlung) are more important.

For both low LET X-rays (50 keV energy) and 1 MeV electrons, the RBE value – needed to evaluate the equivalent dose starting from the physical one in biological tissues - was assumed to be 1.1 [13,37], as in equation (1) for brain, skull and skin tissues.

Monte Carlo Simulation of LEX-IORT and IOERT Treatments

To properly compare the main figures of merit of the nIORT® technique with the standard LEX-IORT and IOERT treatments, the same MCNP geometry and irradiation conditions were considered. By referring to the right side of Figure 2, showing an enlarged drawing of the 4-cm-diameter cylindrical IORT applicator (purple) positioned in the skull "opening":

- while in the nIORT® case the primary 2.45 MeV neutrons are generated almost isotropically in the titanium target (by the 2-cm-diameter D+ beam) and cross the Al holder, the HDPE bearing nose and some air gaps before reaching the superficial tissues of the brain tumor bed;
- in the MCNP simulations of the LEX-IORT and IOERT treatments, the 50 keV X-rays and the 1 MeV focused electrons were generated directly on the external surface of the applicator end-cap and crossed only the 0.2 cm air gap (to consider the tissue irregularities) before reaching the brain tumor bed.

In view of the comparison with the nIORT® performances, the LEX-IORT and IOERT focused beams were assumed with 2 cm diameter size and the same level of particles' flux on the brain surface was imposed: about 1.65 10^8 cm^{-2} s^{-1}. In detail, as shown in Table 1, the X-ray and electron source yield (last column) was tuned to obtain the same flux of primary particles impinging – in the forward direction - on a 2-cm-diameter circular area of the brain superficial tissues at the center of the tumor bed. It can be observed that:

- to obtain the same flux level, the neutron source yield is about 5 times the X-rays and electron ones, mainly because of the different beam spatial distribution (almost isotropic vs. focused);
- in the neutron and X-ray cases the flux in the forward direction is 91-92% of the total, while in the electron case is higher (≅ 96%). Thus, the primary particles are scattered back from the brain tissues to air in different percentages: about 8% in the nIORT® and LEX-IORT cases, and only about 4% in the IOERT one.

Comparison Among nIORT®, LEX-IORT and IOERT Treatments

By assuming the same flux level of incoming primary particles on a 2-cm-diameter brain circular area (see Table 1), the flux values were evaluated in the 2-mm-thick cells representing the superficial tissues of the surgical cavity (i.e., brain, skull and skin) and the 2÷5 mm thick cells in brain depth (see Figure 2). Figure 4a shows the results obtained by the MCNP code in surface tissues: as in Figure 3 they are reported without uncertainties and, as indicated in Figure 2, the "R" axis until 2 cm refers to brain tissues and the last two values refer to the skull and skin cells. It results evident that:

- the focused beams of X-rays and electrons irradiate only the central part of the tumor bed in a 1-cm-radius circular area (corresponding to the beam section), while the diffuse neutron beam irradiates – with decreasing flux levels around the central peak - the whole tissue area in front of the 2-cm-radius applicator end-cap, as well as the skull and skin tissues on its lateral side;
- despite the same integral flux values of impinging particles on surface tissues (see Table 1), the electron flux in the first 2 mm (i.e., thickness of surface cells) is 20-25% higher than the photon flux and the central peak of the neutron flux: evidently, multiple scattering events due to impinging electrons are generated in the first millimeters of brain tissues, resulting in a high LET.

Table 1: MCNP results: flux of primary incident particles on brain surface in a 2-cm-diameter circular area at the centre of tumor bed.

IORT Technique	Incident primary particle	Flux [cm^{-2} s^{-1}]			Fwd / Tot	Source Yield
		Backward	Forward	Total	[%]	[s^{-1}]
nIORT®	Neutron	1.445e7	**1.644e8**	1.789e8	91.9	3.30e9
LEX-IORT	X-ray	1.666e7		1.810e8	90.8	5.14e8
IOERT	Electron	7.119e6		1.715e8	95.8	5.11e8

Figure 4b shows the flux levels in brain depth: as expected, the neutron flux results less penetrating than the X-rays one (for the higher LET) and more penetrating than the electron flux, that

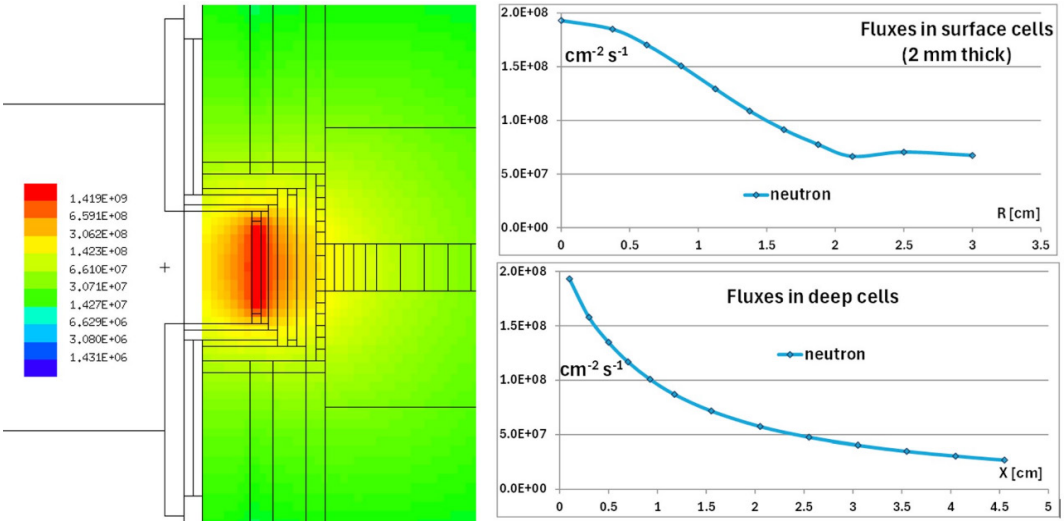

Figure 3: 2D spatial distributions of the neutron flux inside and around the nIORT® applicator (left). Neutron flux in superficial tissues of the surgical cavity around the IORT applicator (top-right) and in brain depth (bottom-right) [cm^{-2} s^{-1}].

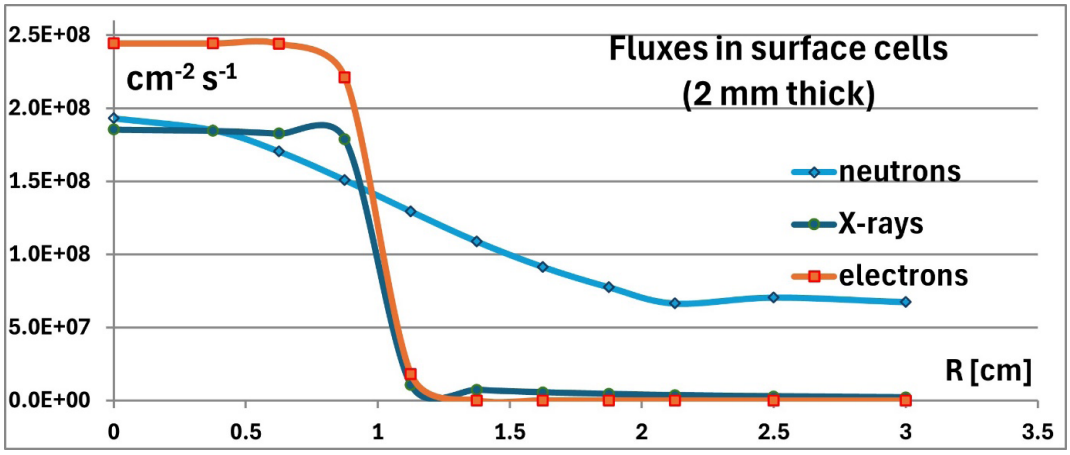

Figure 4a: MCNP results: neutron, X-ray and electron flux values in the superficial tissues of the surgical cavity with nIORT®, LEX-IORT and IOERT techniques (2 mm thick cells; [cm^{-2} s^{-1}]).

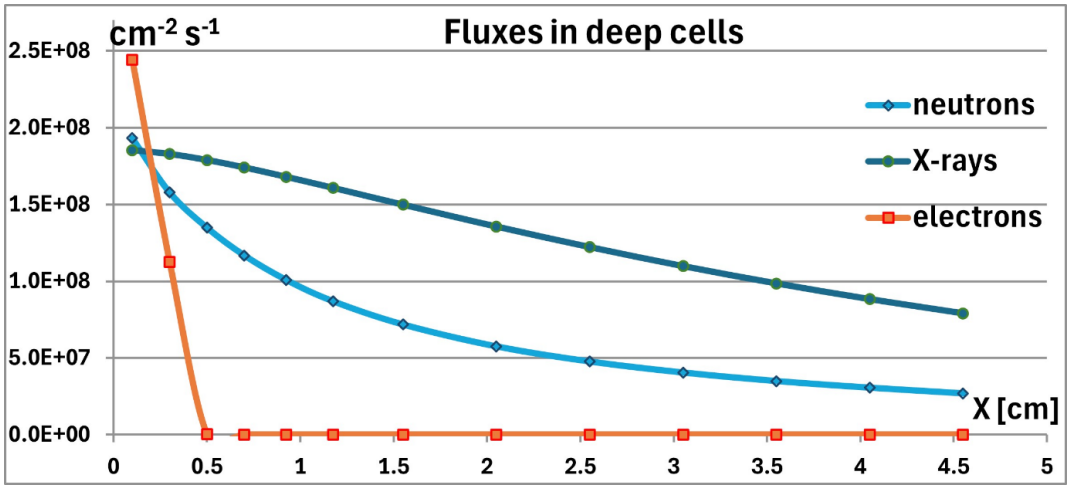

Figure 4b: MCNP results: neutron, X-ray and electron flux values in brain depth with nIORT®, LEX-IORT and IOERT techniques (2÷5 mm thick cells; [cm^{-2} s^{-1}]).

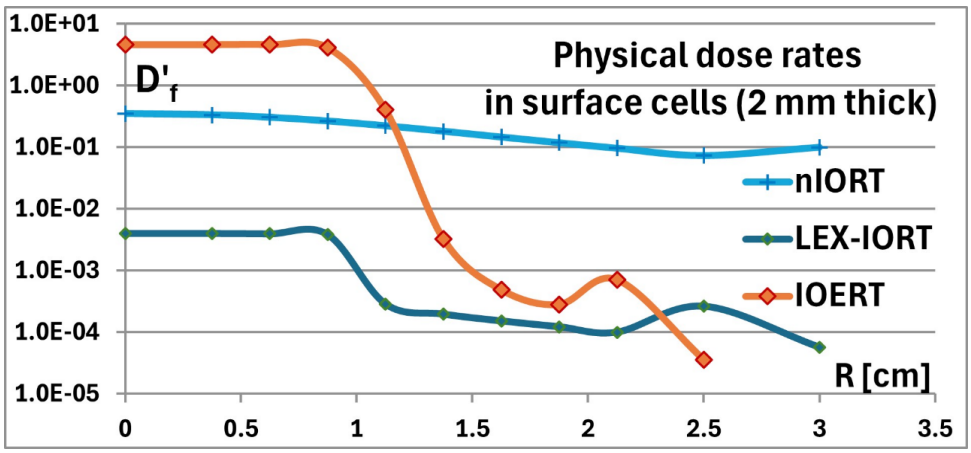

Figure 5a: MCNP results: physical dose rates in the superficial tissues of the surgical cavity with nIORT®, LEX-IORT and IOERT techniques (2 mm thick cells; [Gy/min]).

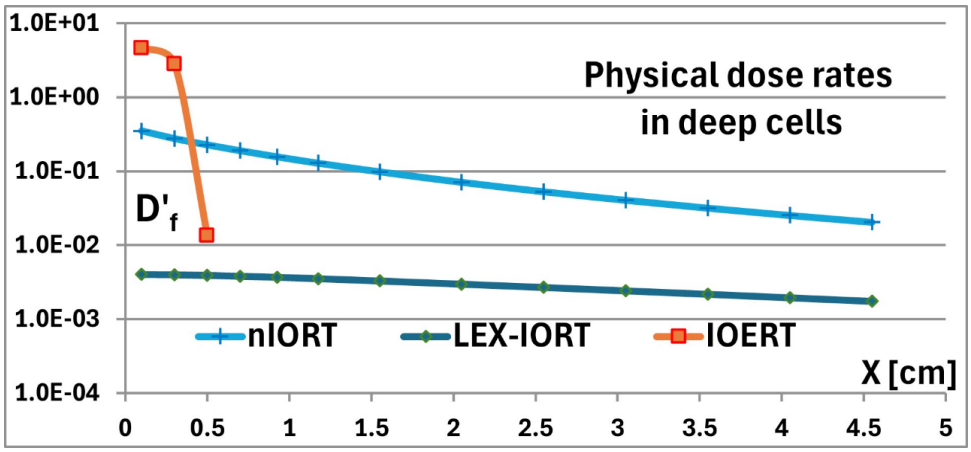

Figure 5b: MCNP results: physical dose rates in brain depth with nIORT®, LEX-IORT and IOERT techniques (2÷5 mm thick cells; [Gy/min]).

drops to zero after 0.6 cm in brain tissues. Even if not shown, it can be mentioned that in the nIORT® case, the flux level of photon secondary particles is in the order of 3-5% in surface tissues and creases at 10% at 5 cm depth.

Figure 5a shows the physical dose rate levels (Gy/min) in the 2-mm-thick cells representing the superficial tissues of the surgical cavity: as for fluxes in Figures 3 and 4a (and indicated in the right part of Figure 2), the values refer to the brain tumor bed until 2 cm radius, while the last two ones refer to the lateral skull and skin cells. As expected, the physical dose rate distributions follow the flux behavior of the diffused neutrons and focused X-rays and electrons. But, despite the same flux level of incoming particles, the dose rate values are largely different (~3 orders of magnitude) because of the very different LET values of primary particles. The maximum physical dose rates at the center of tumor bed result 0.004 / 0.35 / 4.6 Gy/min for X-rays, neutrons and electrons, respectively. It can be highlighted that on the brain superficial tissues in correspondence of the 2-cm-diameter beam area (around the center of the tumor bed):

- the physical dose rates due to X-rays is ≅85 times lower than the neutron one;
- the physical dose rates due to electrons is ≅14 times higher than the neutron one.

The physical dose rate values shown in Figure 5a for neutrons and X-rays include the contribution of the secondary photon and electron particles, respectively. It can be noticed that in the nIORT® case, the contribution of secondary photons to the physical dose rate in superficial tissues is only about 0.5% of the neutrons contribute (vs. 3-5% for flux values).

Figure 5b shows the physical dose rate levels in brain depth. As in the flux profile (see Figure 4b), the IOERT physical dose rate drops to zero after 0.6 cm in brain tissues. The nIORT® physical dose profile is less penetrating than the LEX-IORT one: with neutrons the dose rate values drop by a factor 20 in 5 cm depth, while with X-rays the values decrease only by a factor 2 in the same 5 cm range. It can be further mentioned that in the nIORT® the physical dose rates due to secondary photons at ≅5 cm depth results ≅5% of the neutron one (vs. about 0.5% at tissues surface).

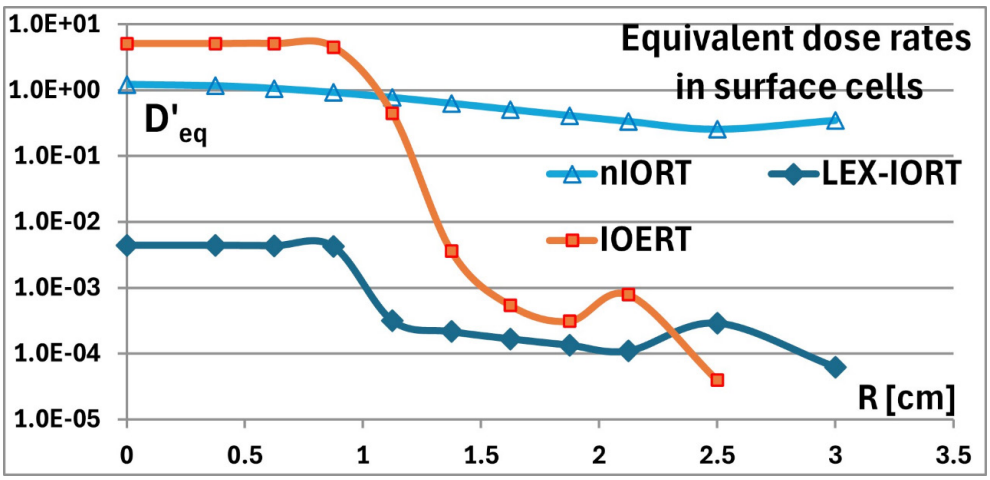

Figure 6a: MCNP results: equivalent dose rates due in the superficial tissues of the surgical cavity with nIORT®, LEX-IORT and IOERT techniques (2 mm thick cells; [Gy(RBE)/min]).

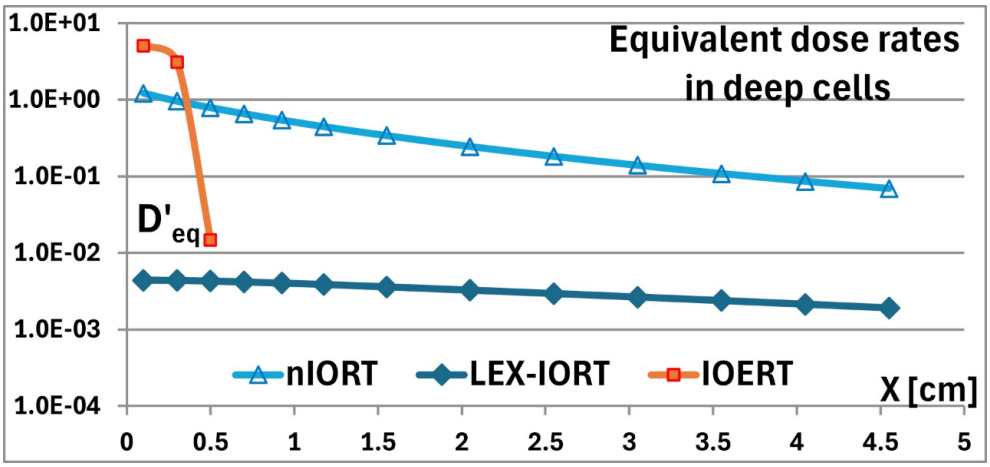

Figure 6b: MCNP results: equivalent dose rates in brain depth with nIORT®, LEX-IORT and IOERT techniques (2÷5 mm thick cells; [Gy/min]).

Figure 6a shows the equivalent dose rate (Gy(RBE)/min) profiles in the 2-mm-thick cells representing the superficial tissues of the surgical cavity: as RBE values, 3.5 was assumed for neutrons and 1.1 for both X-rays and electrons. As in previous graphs in Figures 4a and 5a, the values refer to brain tissues until 2 cm, while the last two refer to the skull and skin cells on the IORT applicator lateral side. Adopting the same flux levels (see Table 1), the LEX-IORT technique provides equivalent dose rates ~ 250 / 1000 times lower than the nIORT® / IOERT ones, respectively: in the nIORT® / IOERT cases, the dose peaks administered at the tissue surface are about 1.2 and 5.1 Gy(RBE)/min, respectively. The physical dose rate due to electrons was about 14 higher than the neutron ones, but the high-RBE of 2.45 MeV neutrons reduces this ratio to about 4. With the almost isotropic neutron beam, the dose rate level decreases smoothly along applicator end-cap radius (reaching ≅20 / 30% of the central peak in the surrounding skull / skin tissues, respectively) and thus should result well suitable for irradiate tumor beds with significant extension.

Figure 6b shows the equivalent dose rates in brain depth. While the equivalent dose due to electrons drops to zero after 0.6 cm in brain tissues, the other two profiles are decisively more penetrating. As for the physical dose profiles (Figure 5b), besides the different orders of magnitude, the LEX-IORT profile decreases in brain depth only by a factor 2 in 5 cm, while the nIORT® profile decreases by a factor 20 in the same 5 cm range. Even if not shown, it can be also mentioned that in nIORT® the equivalent dose rate due to secondary photons in superficial tissues is only ~ 0.15% of the neutrons' contribute, and creases to ~5% at 5 cm depth.

Finally, to highlight the complementary features of the nIORT® treatment in comparison to standard LEX-IORT and IOERT techniques, Figures 7a and 7b shows on a linear scale the normalized dose rate profiles in the superficial tissues of the surgical cavity and in brain depth, respectively. Unlike the previous figures, instead of imposing the same flux of incident primary particles (see Table 1), the same equivalent dose peak was assumed at the center of the tumor bed (e.g., the power of the LEX-IORT device should

be ~250 / 1000 times higher to reach the dose peaks obtained by nIORT® / IOERT, respectively). The peculiar dose profiles provided by the nIORT® device, both at the tissue surface (Figure 7a) and at tissue depth (Figure 7b), could contribute to enhancing the adjuvant treatment of severe cancers with local recurrences, such as GBM. The dosimetry parameters obtained through MCNP refer to brain cancer treatment, but the results could be generalized to other severe solid tumors in different organs and areas of the body.

Discussion

One of the primary advantages of the IORT technique is the elimination of the delay between surgery and adjuvant RT treatments, referred to as the time to initiation. In conventional EBRT techniques, this delay can reduce the efficacy of treatment, especially in cases of GBM brain metastases where potential repopulation within the resection cavity can occur. By eliminating this time gap, IORT modalities - such as the nIORT® - have the potential to provide better outcomes than delayed EBRT approaches by addressing cancer cells immediately after surgical resection, thus minimizing the risk of recurrence. The limited size and weight of the system (~120 kg, manageable remotely by a robotic arm) should make the nIORT® device installable in a hospital OR dedicated to nIORT®, without posing safety and environmental concern, and avoiding the necessity to install an OR in a research center or next to a nuclear reactor.

The feasibility of IORT for brain cancers treatment is largely determined by the accessibility of the tumor bed. While access is easier with small spherical applicators, such as those used in the LEX-IORT technique [12-13], it becomes more challenging with larger cylindrical applicators usually adopted in IOERT [16]. The nIORT® device, with its 4-cm-diameter applicator (see Figure 2), addresses this challenge by allowing efficient irradiation of larger target areas despite the small size of the applicator. Indeed, the neutron's diffusion property further enhances the ability to treat large and irregular tumor volumes. Furthermore, the small size of the applicator makes the nIORT® device potentially suitable for the treatment of many organs and parts of the body.

When selecting the most suitable IORT technique for the solid cancers' treatment, it is essential to consider both the physical characteristics of the irradiating particles and their biological effects on the irradiated tissues. This article compares the nIORT®, LEX-IORT and IOERT techniques by imposing the same flux level of incoming particles on the surface of the irradiated brain tumor bed (see Table 1). In the 50 keV X-rays case, despite the same flux level, the equivalent dose rate in the superficial tissues of the surgical cavity results about 250 / 1000 times lower than the nIORT® / IOERT ones, respectively. Neutrons, as used in nIORT®, offer distinct advantages over traditional X-rays and electrons, particularly due to their higher RBE and LET values. For their high LET, neutrons deliver localized DSBs that are harder to repair and may lead to more effective LTC compared to lower-LET radiation. Furthermore, the 2.45 MeV neutrons have a RBE approximately 3÷5 times higher than X-rays and electrons, making them highly effective in killing cancer cells, including radioresistant ones. The high-LET-RBE particles cause complex DNA damage, which is more difficult for cancer cells to repair: in particular, fast neutrons have been shown to induce cell death in cancer stem cells (CSCs) or metastatic CSCs, which are often responsible for tumor recurrence and metastasis, a key limitation of conventional treatments [20]. The high RBE of fast neutrons makes nIORT® also particularly useful in overcoming the limitations associated with the OER, which is a crucial factor in traditional RT. Neutrons, with a lower OER than X-rays and electrons, are less affected by hypoxic TME, which often hinders the effectiveness of RT [22-23].

Besides the benefits deriving from high-LET-RBE properties, the peculiar spatial dose distributions obtained by fast neutrons lead to other important considerations. Several MCNP studies pointed out that the potential advantages (deriving from the diffuse beam) can be obtained with nIORT® applicators of different shape and size, depending on the organ of the body to be irradiated [38-41]. In the superficial tissues of the surgical cavity, the almost-isotropic diffusion of neutrons allows for effective treatment of irregular tumor beds (see Figures 6a and 7a), without requiring the precise alignment demanded by the standard IORT techniques using focused beams (e.g., by optic systems). Thus, in principle the nIORT® technique could extend the IORT applicability beyond the "focused beam" IOERT and "small target volume" LEX-IORT adjuvant treatments. One of the main peculiarities of the nIORT® is represented by the almost "*spherically symmetric"* field of the beam, in which the neutrons diffusion into the tissues acts as a sort of "particles foam" filling the surgical cavity. The possibility to irradiate extended and irregular tissue area with a diffuse beam could be particularly efficient for the treatment of the GBM tumor, whose diameter at the time of diagnosis is usually ≅4 cm and, in some cases, it reaches up to 10 cm diameter [42]. The isotropic fast-neutron beam should induce necrosis and apoptosis of the QCCs within the topography irregularities of the tumor bed and should allow maximizing LTC by reducing the probability of local recurrences, frequently observed within 2÷3 cm from the GBM initial lesion.

For the dose profiles in brain depth, the nIORT® device delivers a dose gradient not as steep as the IOERT one and, at the same time, not penetrating as LEX-IORT X-rays (see Figure 7b). This feature could be advantageously exploited in balancing the need for effective LTC with minimizing adverse effects on normal tissues and nearest organs at risk (OARs). Even if the dose gradient is not steep as in the IOERT case, the overwhelming part of the nIORT® dose is however administered at brain surface and in the first 3-4 cm in tissue depth (reaching ≅5% of the superficial peak at 5 cm), significantly sparing deeper tissues from excessive radiation.

High-LET-RBE particles could solve also certain clinical challenges related to tissues repair mechanisms, since low-LET radiation typically induces single-strand breaks (SSBs), which

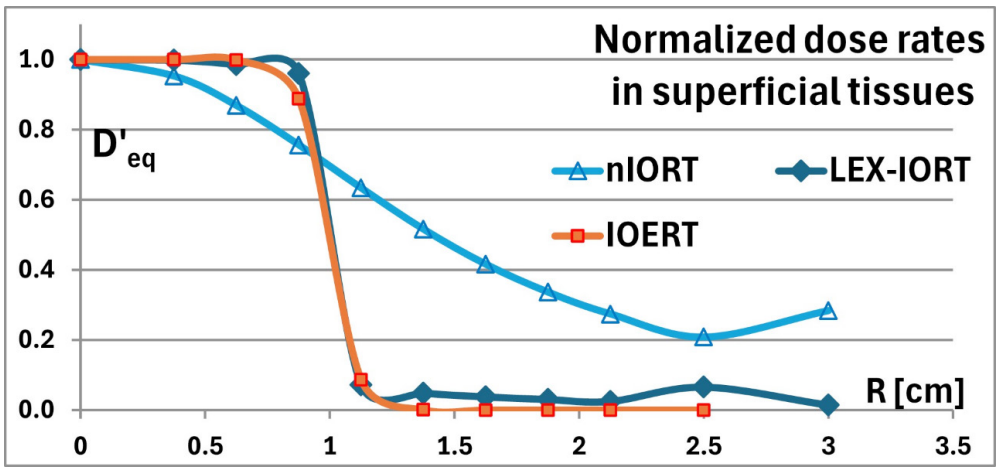

Figure 7a: MCNP results: normalized dose profiles in the superficial tissues of the surgical cavity with nIORT®, LEX-IORT and IOERT techniques (2 mm thick cells).

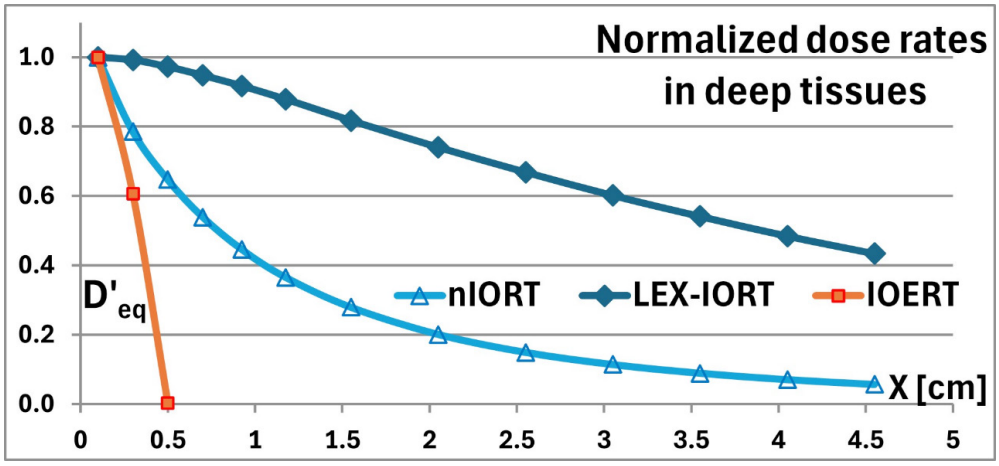

Figure 7b: MCNP results: normalized dose profiles in brain depth with nIORT®, LEX-IORT and IOERT techniques (2÷5 mm thick cells).

are more efficiently repaired by cancer cells through the non-homologous end joining (NHEJ) pathway. In contrast, high-LET radiation like fast neutrons induces more complex DNA lesions, including DSBs, that are harder to repair. This significantly hampers the cancer cells' ability to repair the damage, leading to cell death: indeed, the high-LET-RBE radiation saturates the repair systems of cancer cells at higher doses, leading to genomic instability and potentially greater tumor cell inactivation [43].

For what concerns the potential risks of radiation-induced secondary malignancies (RISMs, [44]), the long-term RISMs have not yet been determined and are difficult to compare with the ones of standard RT techniques [45]. Otherwise, about the radiation-induced bystander effects (RIBE) in which nearby non-irradiated cells experience damage, although RIBE has been observed with X-rays and electron therapies, preclinical studies indicate that neutrons do not induce this phenomenon, which may reduce the risk of unintended damage to healthy tissues [46]. Additionally:

- thanks to the epithermal and thermal tails of the neutron flux spreading out around the tumor bed, the nIORT® could lead to the potential appearance of the radiation induced abscopal effect (RIAE) on distant non-irradiated cells due to the adaptive immune system [47];
- the ability of fast neutrons to inhibit tumor cells proliferation and epithelial-mesenchymal transition (EMT) in GBM and other cancers is a promising area for further exploration, as EMT is a key factor contributing to tumors' metastasis and radio-resistance [48,49].

Although these hypotheses require validation through *in vitro* and *in vivo* preclinical studies, the promising features of nIORT® suggest it could become a valuable addition to the standard-of-care treatments for GBM and other brain malignancies. But, when managing neoplasms with metastatic potential, a purely local approach may be insufficient. The addition of concurrent or adjuvant chemotherapy - such as TMZ [50] - in combination with nIORT® could offer an effective strategy to overcome glioma stem cell resistance, by further improving treatment outcomes. It is known that in case of the standard IORT after surgical resection and adjuvant chemotherapy treatment, about 80-85% of recurrences occur near the resection margins and, even by adding target therapy with bevacizumab, nimotuzumab or cilengitide, the

clinical outcomes are not significantly improved [12]. Instead, because of its superiority in improving necrosis and apoptosis of the tumor cells in the resection margins, the nIORT® regimen should lead to a reduction in recurrences, as long as the fast neutrons' LET is not such as to induce secondary malignancies or an excessive reaction of the adaptation immune system. A possible protocol for the successful treatment of the GBM and other tumors (e.g., breast cancer [39]) could include the nIORT® irradiation delivered immediately after excision, followed by adjuvant EBRT treatments with or without chemotherapy in the TMZ regimen. The most suitable nIORT® irradiation protocol will only be determined by *in vivo* tests or over organoid cultures, as pre-clinical models of the irradiated organs.

Recent studies have highlighted the potential of combining the IORT techniques with immunotherapy [51,52] with some specific applications for the GBM treatment [53-55]. The high RBE of fast neutrons could further enhance immune modulation, stimulating both innate and adaptive immune responses in patients with GBM. This combination may lead to a more robust anti-tumor response, potentially improving patient survival. Clinical evidence supporting the synergistic effect of RT and ICIs is growing, and nIORT® could further amplify this effect by the increased RBE value from 1.1 (for photons and electrons) up to 3÷5, thereby potentially enhancing the immune system's response to the tumor. The potential benefits of ICIs, such as Pembrolizumab and Nivolumab, could be investigated as adjuncts to the single-session nIORT® treatment since these agents may help to overcome tumor-induced immune evasion mechanisms and to enhance the systemic antitumor immune response initiated by neutron-based RT. Indeed, high-LET irradiation can induce extensive cell death within the tumor, creating large quantities of dying or dead cancer cells and associated antigens.

While the abovementioned aspects are beneficial for triggering an antitumor immune response, there is a concurrent risk that macrophages may become saturated by rapidly engulfing tumor debris, thereby impairing their scavenger receptor functions. This potential reduction in the clearance capacity of the immune system underscores the importance of determining an optimal nIORT® irradiation dose that maximizes tumor cell kill but avoids overwhelming macrophages [56,57]. The process of their clearance by efferocytosis via macrophages and dendric cells should be considered to avoid an excess of engulfment phenomenon in the homeostasis processes. Efferocytosis also induces an immunosuppressive TME and hence stimulate the cancer cells of escaping from immune surveillance. In the GBM case, it is known that efferocytosis contributes to the immunosuppressive phenotype of macrophages in this cancer, but a better understanding is needed [58].

Conclusions and Future Perspectives

The nIORT® technique, utilizing fast neutrons produced by a compact generator, represents a promising adjuvant treatment of severe brain cancers - as the GBM - following maximal surgical resection. Differently from the boron neutron capture therapy [60] exploiting thermal and epithermal neutrons to induce (n,α) reactions in boron carriers injected into the patients, the fast neutrons interact directly and efficiently with the hydrogen nuclei, producing recoil protons that ionize the tissues. The IORT approach eliminates the time delay between surgery and RT, offering the potential for improved outcomes compared to traditional EBRT, where tumor repopulation and radio-resistance can diminish treatment efficacy. The system's ability to administer high dose targets within few minutes - e.g., 10÷20 Gy(RBE) in about 8÷16' - further supports its feasibility for clinical use. The utilization of a compact source device - without posing safety concerns - represents another fundamental advantage in the view of possible treatments in a hospital OR dedicated to nIORT®.

The nIORT® technique represents a promising modality for treating GBM and other brain cancers, offering several potential advantages over traditional RT approaches. Its ability to deliver high doses of radiation in a single session, combined with the high LET and RBE (≅3÷5) values of fast neutrons could be highly effective in targeting cancer cells, including radioresistant and motile CSCs, with minimal damage to surrounding healthy tissues in which the RBE value results lower. The high-LET and high-RBE of nIORT® should create a high number of dead and apoptotic tumor cells with respect to the other forms of ionizing radiation fields, such as photons, electrons and protons.

Neutron diffusion allows for treatment of irregularly shaped tumor beds, providing coverage even in complex surgical cavities. The reduced OER and high RBE values of neutrons enhance the efficacy in hypoxic areas of tumors, a limitation for conventional RTs with X-rays and electrons. The spatial dose distribution in surface tissues permits to irradiate larger area of the surgical cavity (with potential local recurrences) in comparison with the LEX-IORT and IOERT techniques exploiting focused beams. The dose profiles in brain depth show complementary properties of the nIORT® treatment in comparison to the standard ones, with a behavior not steep as the IOERT one and not penetrating as the LEX-IORT X-rays. Certainly, LEX-IORT and IOERT have well-established protocols, are easier to manage and offer precision in dose delivery with predictable outcomes. But the development of the nIORT® technique could integrate these standard techniques especially for tumor beds with significant extension, topographic irregularities and possible local recurrence - as the GBM - that remain a therapeutic challenge. The dosimetry parameters obtained by the MCNP code refer to the brain cancers treatment, but the results could be generalized to sever solid tumors in other organs. Indeed, the limited size of the nIORT® applicator (4-cm diameter) allows to reach the major parts of the body: even the internal organs could be also irradiated by adopting standard surgical spacers, e.g., as for the locally advanced pancreatic cancers [59].

Future studies should explore the feasibility of leveraging nIORT® to prime the immune response, potentially followed by sessions of EBRT to sustain immune system activation over time: this strategy could mitigate tumor recurrence and improve long-term control. Even if further pre-clinical and clinical studies

are required to evaluate these combined strategies - particularly in terms of safety, efficacy and optimal timing - this approach holds significant promise for improving treatment outcomes and survival rates for patients with GBM and other severe brain malignancies. With further clinical validation, nIORT® could become a standard adjuvant treatment, potentially in combination with chemotherapy and/or immunotherapy, providing a more effective and personalized approach to brain cancer therapy. Emerging evidence highlights the synergic potential of combining RT with immunotherapy to improve patient outcomes, since RT can enhance immunogenic cell death and can promote the release of tumor antigens activating the immune system. The integration of nIORT® with immunotherapeutic modalities represents an exciting frontier in the multidisciplinary management of aggressive brain tumors and could provide a unique opportunity to "educate" the immune system to recognize and target solid tumors more effectively. Future investigations should focus on establishing dose–response parameters that balance potent local control and immunogenic stimulation, with minimal immunosuppressive effects resulting from macrophage saturation. Such dose-optimization studies will be critical to fully integrate nIORT® with emerging immunotherapeutic strategies, including immune checkpoint blockade, to achieve both local control and systemic antitumor effects.

Acknowledgements

TheranostiCentre acknowledges the valuable contributions of its CEO, Dr. Paolo Galmozzi, whose leadership has positively influenced this research. Additionally, the pivotal role of ENEA in supporting and promoting this study is duly recognized, with special thanks extended to Drs. Antonietta Rizzo and Giuseppe Ottaviano of ENEA for their efforts in facilitating the installation of the compact neutron generator at the ENEA Research Center in Brasimone (Bologna).

The computing resources for this work have been provided by CRESCO/ENEAGRID High Performance Computing infrastructure (funded by ENEA and by Italian and European research programs) and its staff (see http://www.cresco.enea.it for information).

References

1. Davis ME. Glioblastoma: Overview of Disease and Treatment. Clin J Oncol Nurs. 2016; 20: S2-S8.
2. Wu W, Klockow JL, Zhang M, et al. Glioblastoma multiforme (GBM): an overview of current therapies and mechanisms of resistance. Pharmacol Res. 2021; 171.
3. Goenka A, Tiek D, Song X, et al. The Many Facets of Therapy Resistance and Tumor Recurrence in Glioblastoma. Cells. 2021; 10: 484.
4. Gaillard F, Campos A, Kogan J, et al. Stupp protocol. Reference article, Radiopaedia.org Nov. 2024.
5. Koosha F, Ahmadikamalabadi M, Mohammadi M. Review of Recent Improvements in Carbon Ion Radiation Therapy in the Treatment of Glioblastoma. Adv Radiat Oncol. 2024 ;9: 101465.
6. Rajpurohit YS, Sharma DK, Lal M, et al. A perspective on tumor radiation resistance following high-LET radiation treatment. J Cancer Res Clin Oncol. 2024; 150: 226.
7. Alhmoud JF, Woolley JF, Al Moustafa AE, et al. DNA Damage/Repair Management in Cancers. Cancers. 2020; 12: 1050.
8. Crittenden M, Kohrt H, Levy R, et al. Current clinical trials testing combinations of immunotherapy and radiation. Semin Radiat Oncol. 2015; 25: 54-64.
9. Riva G, Pecorari G. Multimodality and Sequential Therapy in Locally Advanced Head and Neck Cancer: A Preface to the Special Issue. Cancers. 2021; 13: 2609.
10. Hensley FW. Present State and Issues in IORT Physics. Radiat Oncol. 2017; 12: 37.
11. Hashemi S, Javadi S, Mirzaei H, et al. Comparison of IORT (Radical and Boost Dose) and EBRT in Terms of Disease-Free Survival and Overall Survival according to Demographic, Pathologic, and Biological Factors in Patients with Breast Cancer. Int J Surg Oncol. 2021; 2476527.
12. Ylanan AMD, Pascual JSG, Cruz-Lim EMD, et al. Intraoperative radiotherapy for glioblastoma: A systematic review of techniques and outcomes. J Clin Neurosci. 2021; 93: 36-41.
13. Giordano FA, Abo Madyan Y, Brehmer S, et al. Intraoperative radiotherapy (IORT) - a resurrected option for treating glioblastoma? Translational Cancer Research. 2014; 3.
14. Wu W, Klockow JL, Zhang M, et al. Glioblastoma multiforme (GBM): an overview of current therapies and mechanisms of resistance. Pharmacol Res. 2021; 171.
15. Cifarelli CP, Jacobson GM. Intraoperative Radiotherapy in Brain Malignancies: Indications and Outcomes in Primary and Metastatic Brain Tumors. Front Oncol. 2021; 11.
16. Usychkin S, Calvo F, Samblás J, et al. Intra-Operative Electron Beam Radiotherapy for Newly Diagnosed and Recurrent Malignant Gliomas: Feasibility and Long-Term Outcomes. Clin. Transl. Oncol. 2013; 15: 33-38.
17. Cifarelli CP, Brehmer S, Vargo JA, et al. Intraoperative Radiotherapy (IORT) for Surgically Resected Brain Metastases: Outcome Analysis of an International Cooperative Study. J Neurooncol. 2019; 145: 391-397.
18. Giordano FA, Brehmer S, Mürle B, et al. Intraoperative Radiotherapy in Newly Diagnosed Glioblastoma (INTRAGO): An Open-Label, Dose-Escalation Phase I/II Trial. Neurosurgery. 2019; 84: 41-49.
19. Leung KG. New compact neutron generator system for multiple applications. Nuclear Tech. 2020; 206: 1-8.
20. Bleddyn J. Clinical Radiobiology of Fast Neutron Therapy: What Was Learnt? J Front Oncol. 2020; 10.
21. Kiragga F, Brazovskiy K. Exploiting the unique interaction characteristics of fast neutrons for improved cancer therapy: A radiobiological perspective. Radiation Medicine and Protection. 2024; 5: 24-29.

22. Antonovic L, Lindblom E, Dasu A, et al. Clinical oxygen enhancement ratio of tumors in carbon ion radiotherapy: the influence of local oxygenation changes. J Radiat Res. 2014; 55: 902-911.
23. Rini F, Hall EJ, Marino SA. The Oxygen Enhancement Ratio as a Function of Neutron Energy with Mammalian Cells in Culture. Radiat Res. 1979; 78: 25-37.
24. Karen KF, Theodore LP, Jay RR. The RBE of neutrons in vivo. Cancer. 1974; 34: 48-53.
25. Dousset MH, Hamard J, Ricourt A. Distribution of the dose from neutrons in a thin sample of wet tissue as a function of linear energy transfer (LET). Phys Med Biol. 1971; 16: 467-478.
26. Stewart RD, Anderson A, Sandison G, et al. O 05 - Comparative analysis of neutron relative biological effectiveness (RBE) for clinical, cellular and molecular endpoints. Int J of Particle Therapy. 2024; 11.
27. Martellini M, Gherardi G. Apparatus for the intraoperative radiotherapy. European Patent 2019; EP 3 522 177 B1.
28. Obrador E, Moreno-Murciano P, Oriol-Caballo M, et al. Glioblastoma Therapy: Past, Present and Future. Int J Mol Sci. 2024; 25: 2529.
29. Pelowitz B. MCNP6 user's manual. Tech. Rep. Los Alamos National Lab 2013; LA-CP-13-00634 Rev. 0.
30. Obložinský P. Special Issue on Nuclear Data. Nuclear Data Sheets. 2018; 148: 1-420.
31. Martellini M, Gherardi G, Leung K, et al. Multi Purpose Compact Apparatus for the Generation of a high-flux of neutrons, particularly for Intraoperative Radiotherapy. Int. Patent. 2021.
32. Laboratorio per la caratterizzazione di Irradiatori Neutronici Compatti in Emilia Romagna. LINCER project funded by Emilia Romagna with "Legge Regionale 27/12/2018 N.25, DGR N. 545/2019 – CUP I74I19000360003". 2020-2022.
33. Zankl M, Williams G, Drexler G, et al. The calculation of dose from external photon exposures using reference human phantoms and Monte-Carlo: part I. The male (Adam) and female (Eva) adult mathematical phantom. Tech. Report GSF. 1982; S-885.
34. Jones B. Fast neutron energy based modelling of biological effectiveness with implications for proton and ion beams. Phys Med Biol. 2021; 66: 045028.
35. Gunderson LL, Tepper JE. Clinical Radiation Oncology 2012. Book 3rd Edition. ISBN 978-1-4377-1637-5. https://www.sciencedirect.com/book/9781437716375/clinical-radiation-oncology
36. ICRU report 16. Linear Energy Transfer. International Commission on radiation units and measurements. 1970.
37. Marthinsen AB, Gisetstad R, Danielsen S, et al. Relative Biological Effectiveness of Photon Energies Used in Brachytherapy and Intraoperative Radiotherapy Techniques for Two Breast Cancer Cell Lines. Acta Oncol. 2010; 49: 1261-1268.
38. Martellini M, Sarotto M, Leung K, et al. A Compact Neutron Generator for the nIORT® Treatment of Severe Solid Cancers. Medical Research Archives. 2023; 11.
39. Martellini M, Sarotto M, Leung K, et al. Feasibility Study on the nIORT® Adjuvant Treatment of Brain and Breast Cancers by Fast Neutrons produced by a DD-fusion Compact Generator. Am J Biomed Sci & Res. 2024; 22: 577-579.
40. Martellini M, Sarotto M, Leung K, et al. Feasibility Study on the nIORT® Adjuvant Treatment of Glioblastoma Multiforme through the Irradiation Field of Fast Neutrons Produced by a Compact Generator. Am J Biomed Sci & Res. 2024;12.
41. Sarotto M, Martellini M. MCNP analyses of the 100 kV D-ion-based compact neutron source: irradiation performances for nIORT® treatments with different irradiation window diameters. Tech Rep ENEA. 2022; SICNUC-P000-045. https://iris.enea.it/handle/20.500.12079/60152
42. Urbańska K, Sokołowska J, Szmidt M, et al. Glioblastoma multiforme - an overview. Contemp Oncol (Pozn). 2014; 18: 307-312.
43. Busato F, El Khouzai B, Mognato M. Biological Mechanisms to Reduce Radioresistance and Increase the Efficacy of Radiotherapy: State of the Art. Int J Mol Sci. 2022; 23.
44. Burt LM, Ying J, Poppe MM, et al. Risk of secondary malignancies after radiation therapy for breast cancer: comprehensive results. Elsevier J. the Breast. 2017; 35: 122-129.
45. Newhauser WD, Durante M. Assessing the risk of second malignancies after modern radiotherapy. Nat Rev Cancer. 2011;11: 438-48.
46. Wang C, Smith RW, Duhig J, et al. Neutrons do not produce a bystander effect in zebrafish irradiated in vivo. Int J Radiat Biol. 2011; 87: 964-973.
47. Trivillin VA, Pozzi EC, Colombo LL, et al. Abscopal effect of boron neutron capture therapy (BNCT): proof of principle in an experimental model of colon cancer. Radiat Environ Biophys. 2017; 56: 365-375.
48. Gapanova AV, Rodin S, Mazina AA, et al. Epithelial–Mesenchymal Transition: Role in Cancer Progression and the Perspectives of Antitumor Treatment. Acta Naturae. 2020; 12: 4-23.
49. Roche J. The Epithelial-to-Mesenchymal Transition in Cancer. Cancers. 2018; 10.
50. Singh N, Miner A, Hennis L, et al. Mechanisms of temozolomide resistance in glioblastoma-a comprehensive review. Cancer Drug Resist. 2021; 4: 17-43.
51. Kumari S, Mukherjee S, Sinha D, et al. Immunomodulatory Effects of Radiotherapy. Int J Mol Sci. 2020; 21.
52. Chi A, Nguyen NP. Mechanistic rationales for combining immunotherapy with radiotherapy. Front Immunol. 2023; 14.
53. Awada H, Paris F, Pecqueur. Exploiting radiation immunostimulatory effects to improve glioblastoma outcome. Neuro Oncol. 2023; 25: 433-446.

54. Gillette JS, Wang JE, Dowd RS, et al. Barriers to overcoming immunotherapy resistance in glioblastoma. Front Med. 2023; 10.

55. Layer JP, Shiban E, Brehmer S, et al. Multicentric assessment of safety and efficacy of combinatorial adjuvant brain metastasis treatment by intraoperative radiotherapy and immunotherapy. Int J Radiat Oncol Biol Phys. 2024; 118: 1552-1562.

56. Ian A J Lorimer. Potential roles for efferocytosis in glioblastoma immune evasion. Neurooncol Adv. 2024; 6: vdae012.

57. Qiu H, Shao Z, Wen X, et al. Efferocytosis: An accomplice of cancer immune escape. Biomed Pharmacother. 2023; 167: 115540.

58. Gao M, Huang J, Yang B, et al. Identification of efferocytosis-related subtypes in gliomas and elucidating their characteristics and clinical significance. Front Cell Dev Biol. 2023; 11.

59. Lee D, Komatsu S, Terashima K, et al. Surgical spacer placement for proton radiotherapy in locally advanced pancreatic body and tail cancers: initial clinical results. Radiat Oncol. 2021; 16: 3.

60. Nishitani T, Yoshihashi S, Tanagami Y, et al. Neutronics Analyses of the Radiation Field at the Accelerator-Based Neutron Source of Nagoya University for the BNCT Study. Nucl Eng. 2022; 3: 222-232.